

Effects of Ray-Tracing on Apparent Initial Directivity of Rocket Noise Measurements

Nathan Carlston

A senior thesis submitted to the faculty of
Brigham Young University
in partial fulfillment of the requirements for the degree of

Bachelor of Science

Kent Gee, Advisor

Department of Physics and Astronomy

Brigham Young University

Copyright © 2026 Nathan Carlston

All Rights Reserved

ABSTRACT

Effects of Ray-Tracing on Apparent Initial Directivity of Rocket Noise Measurements

Nathan Carlston

Department of Physics and Astronomy, BYU

Bachelor of Science

Rocket launches produce high-intensity noise that can affect nearby communities, wildlife, and structures. Predicting this noise accurately at short distances is challenging because atmospheric effects, such as temperature and wind gradients, can bend sound waves. This alters their apparent directivity, meaning the direction from which sound appears to originate when inferred from measurements. In this study, we apply a Hamiltonian-based ray-tracing framework to model acoustic propagation from rocket launches within the first five kilometers of the atmosphere. Using an iterative eigenray solver, we compute acoustic paths connecting the launch trajectory to 56 receiver stations positioned along eight azimuthal directions at distances ranging from 1 to 15 km from the launch pad, under diurnal atmospheric conditions. These results are compared to traditional straight-line propagation models to quantify the impact of atmospheric refraction on apparent directivity and it is shown that the average deviation in apparent directivity between straight-line and ray-traced models is 2.58° . Even at low altitudes and short ranges, refraction produces measurable deviations in predicted launch angles, with temperature gradients primarily driving mean differences and wind gradients contributing to directional variability. These findings demonstrate that incorporating ray-tracing methods can change apparent directivity even in short range conditions where a constant atmosphere is typically assumed.

Keywords: Rocket Noise, Ray Tracing, Atmospheric Refraction, Source Modeling, Sound Propagation Modeling, Linear Acoustics

ACKNOWLEDGMENTS

I would like to sincerely thank my research advisor, Dr. Kent Gee, for his guidance, insightful feedback, and encouragement throughout this project. His expertise in acoustics and dedication to mentoring have been invaluable in shaping both this research and my development as a scientist.

I also extend my gratitude to the faculty and staff of the BYU Department of Physics and Astronomy, and the College of Computational, Mathematical, and Physical Sciences, for providing a supportive academic environment and the resources necessary to conduct this research.

Finally, I wish to thank my peers, friends, and family for their encouragement and support throughout the thesis process.

Contents

Table of Contents	iv
List of Tables	v
List of Figures	v
1 Introduction	1
2 Methods	3
2.1 Ray Tracing Framework	3
2.1.1 Solving the Eikonal Equation	3
2.2 Iterative Ray Shooting Method for Eigenrays	5
2.3 Simulation	7
3 Results	9
3.0.1 Range Dependence	10
4 Discussion	12
4.1 Sources of Uncertainty	13
5 Conclusion	14
Bibliography	15
Index	18

List of Tables

3.1	Mean and standard deviation of angular deviation between straight-line propagation and ray-traced eigenrays for receiver stations at various distances from the launch pad. Values are calculated for rays within the 60–80° launch angle range.	11
-----	--	----

List of Figures

2.1	Comparison of sound propagation paths from a rocket launch. Blue lines show eigenrays computed using ray tracing through a vertically stratified atmosphere, while red lines represent straight-line rays assuming a constant atmosphere. Atmospheric refraction produces noticeable curvature and influences apparent directivity	6
2.2	Layout of the 56 simulated receiver stations around the launch pad at Vandenberg Space Force Base. Stations are positioned along eight azimuthal directions (N, NE, E, SE, S, SW, W, NW) at distances from 1 km to 15 km. This configuration allows analysis of apparent directivity across range with a representative collection of stations in the azimuth.	8
3.1	Histogram of angular deviations between straight-line propagation and ray-traced eigenrays for rays within the 60–80° launch angle range. Positive values indicate rays bent upward, and negative values indicate downward bending relative to the straight-ray assumption. The mean deviation is 2.58°, demonstrating measurable atmospheric effects even at short ranges.	10

Chapter 1

Introduction

In recent years, the number of rocket launches has increased substantially [1]. This raises concerns about the impact of launch noise on nearby communities, wildlife, and structures [2] [3] [4]. Developing accurate predictive models for rocket noise is essential both for understanding these effects and to reduce the impact of rocket noise on their environments. In order to predict rocket noise at a given location, one needs to have both a source model (how the sound is generated) and a propagation model (how the sound spreads out from the source).

At short distances from the pad, it is common for a simplified straight-line propagation model to be used [5] [6]. This is equivalent to assuming a constant atmosphere with no wind or temperature gradients. While simple and easy to calculate, this model ignores any propagation effects caused by a non-uniform atmosphere. Atmospheric sound propagation is strongly influenced by spatial variations in temperature and wind which cause atmospheric refraction. The acoustic wave equation governs how sound propagates and, when taken to the high frequency limit, reduces to the standard Eikonal equation which describes the travel path of light rays, or, in the high frequency limit, sound rays. Ray-tracing is a method used in both optical and geometric acoustics to solve the Eikonal equation. Ray-tracing methods are widely used to account for refraction in nonuniform

atmospheres [7]. Ray-tracing methods, however, are typically applied only to longer-range acoustic predictions because it is commonly assumed that the effects at short distances are negligible.

In this work, our objective is to quantify the validity of this assumption at different distances from the launch pad. We apply ray-tracing techniques to calculate propagation paths at close ranges and low altitudes. We compare straight-line propagation models with ray-tracing propagation models for acoustic rays initiating within the first five kilometers of the atmosphere. The effect of the straight-ray assumption on perceived acoustic directivity is analyzed, and we show that even at relatively short distances and low altitudes, atmospheric refraction can noticeably shift the implied directivity pattern.

These results demonstrate that straight-line propagation assumptions can lead to meaningful discrepancies in apparent directivity. Since acoustic source models are directivity dependent, different apparent directivity angles lead to different predicted levels and different interpretation of measured data. Incorporating ray-tracing effects at short ranges can therefore improve the prediction of rocket noise and contribute to the development of more accurate and physically consistent rocket noise models from measured acoustic data.

Chapter 2

Methods

2.1 Ray Tracing Framework

This section describes the mathematical and numerical framework used to model the propagation of acoustic rays in a stratified atmosphere. The governing equations, the modeling assumptions, and the numerical implementation are presented in the following subsections.

2.1.1 Solving the Eikonal Equation

In the high-frequency limit, the acoustic wave equation reduces to the Eikonal equation,

$$|\nabla T(\mathbf{r})|^2 = \frac{1}{c_{eff}^2(\mathbf{r})}, \quad (2.1)$$

where $T(\mathbf{r})$ is the travel time and $c_{eff}(\mathbf{r})$ is the effective sound speed; both of these depend on \mathbf{r} , the position vector.

The Eikonal equation can be efficiently solved using the Hamiltonian formulation. We begin by defining our Hamiltonian as

$$H(\mathbf{r}, \mathbf{p}) = \frac{1}{2} ((1 - \mathbf{p} \cdot \mathbf{v})^2 - c^2(\mathbf{r})|\mathbf{p}|^2) \quad (2.2)$$

where $c(r)$ is thermodynamic sound speed, $\mathbf{v}(r)$ is wind velocity, and \mathbf{p} is the slowness vector which has magnitude of the inverse of effective sound speed and direction of effective sound speed. The Eikonal equation can then be written as a canonical system of first-order ordinary differential equations,

$$\frac{d\mathbf{r}}{dt} = \frac{\partial H}{\partial \mathbf{p}}, \quad \frac{d\mathbf{p}}{dt} = -\frac{\partial H}{\partial \mathbf{r}}, \quad (2.3)$$

where \mathbf{r} is the position vector and t is travel time along the ray. This formulation allows for straightforward integration using standard ODE numerical methods.

In order to solve this equation, we need both thermodynamic sound speed and wind velocity as a function of position. In the present work, the atmosphere was assumed to be horizontally homogeneous but vertically stratified so that all atmospheric properties vary only with altitude. This assumption is commonly adopted in outdoor sound propagation problems and is justified by the lack of significant horizontal inhomogeneity on the spatial scales of interest. Under this assumption, the Hamiltonian system reduces to the following set of equations

$$\mathbf{s} = \frac{\mathbf{n}}{c + \mathbf{n} \cdot \mathbf{v}}, \quad (2.4)$$

$$\frac{ds_z}{dt} = -\frac{\Omega}{c} \frac{dc}{dz} - \mathbf{s}_\perp \cdot \frac{d\mathbf{v}_\perp}{dz}, \quad (2.5)$$

$$\Omega = 1 - \mathbf{v}_\perp \cdot \mathbf{s}_\perp, \quad (2.6)$$

$$\frac{d\mathbf{r}}{dt} = c\mathbf{n} + \mathbf{v} = \frac{c^2}{\Omega} \mathbf{s} + \mathbf{v}. \quad (2.7)$$

where \mathbf{r} is the position vector, \mathbf{n} is the unit vector in the ray direction, \mathbf{s} is the slowness vector, and \perp denotes the horizontal components [7] [8].

Since the slowness components along x and y are constant, this formulation reduces the full 6-dimensional Hamiltonian system to a 4-dimensional system (3 position dimensions plus 1 slowness component), reducing computation cost when compared to the full 6-D system [8].

To solve the ray-tracing equations, accurate atmospheric parameters are required. Weather data were obtained from NOAA's Integrated Global Radiosonde Archive, which provides wind speed, wind direction, and temperature profiles from weather balloons [9]. Balloons are released at Vandenberg SFB (the rocket launch site) every day. Although the measurements are altitude-only, they are sufficient for the homogeneous stratified atmospheric model used here. Atmospheric input parameters for the simulation were obtained from weather balloons launched in diurnal conditions.

The raw weather data were interpolated onto a uniform altitude grid and filtered with a low-pass Butterworth filter to reduce high-frequency noise and non-physical measured values due to turbulence in the planetary boundary layer. To ensure smooth derivatives and avoid numerical artifacts in the ray-tracing solver, the interpolated profiles were further smoothed using a Savitzky–Golay filter with a low-order polynomial and a small window length.

The equations of motion were integrated using MATLAB's ode45 variable-step Runge–Kutta solver, which provides a balance between accuracy and computational efficiency. Step sizes are automatically adapted by the solver to maintain error control. Rays were launched with prescribed initial polar and azimuthal angles, and the integration proceeded until the ray either reached the ground or exceeded the range of the receiver. This numerical implementation of the Eikonal equation is what allows us to calculate the sound propagation path through the atmosphere.

The ray-tracing code was validated against a published ray-tracing code producing relative error of $< 0.001\%$ for calculated travel paths across a variety of simulated atmospheric conditions. [10].

2.2 Iterative Ray Shooting Method for Eigenrays

An eigenray is a ray that directly connects a source to a receiver. These rays are of interest because they provide information about the arrival time of sound from a source to a receiver and the path it follows. In this paper, we are interested in finding eigenrays connecting the rocket (acoustical

source) to a particular location (receiver). Knowing the path sound takes is critical to understanding differences in apparent directivity that arise from taking the ray-traced path as opposed to taking a straight-line path from the constant atmosphere assumption.

Figure 2.1 shows an example of the differences between ray-traced and straight eigenrays.

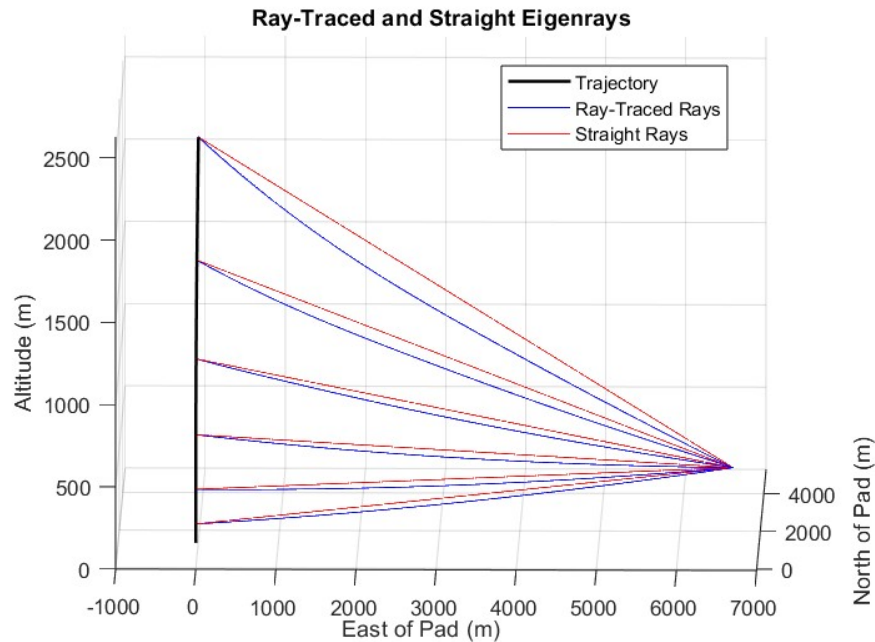


Figure 2.1 Comparison of sound propagation paths from a rocket launch. Blue lines show eigenrays computed using ray tracing through a vertically stratified atmosphere, while red lines represent straight-line rays assuming a constant atmosphere. Atmospheric refraction produces noticeable curvature and influences apparent directivity

Finding eigenrays requires finding the exact initial conditions of a ray that will cause it to intersect a final point. The initial position is given by the position of the rocket at some point in time. This leaves us with undetermined initial conditions for the slowness vector. To find eigenrays, we used an iterative shooting method that involved shooting a ray with specified initial slowness, calculating its travel path, and then adjusting the initial slowness based on the miss between the ray's travel path and the desired receiver. This approach allows us to find the initial slowness needed in order to cause the ray to intersect a receiver.

To efficiently identify eigenrays connecting a source to a given receiver, initial rays are launched from the source with a range of polar and azimuthal angles. The endpoints of these rays are calculated, and the solver checks whether the receiver lies within the angular range spanned by the rays. If the receiver does not lie within this range, the angular span is adjusted. A new ray is then launched at an intermediate angle between the rays that straddle the receiver. This iterative procedure is first applied in the polar direction, then in the azimuth, and the process alternates between polar and azimuthal refinement until a solution ray reaches the receiver within the specified tolerance. After each refinement in one angular direction, the iterative procedure is applied to the other. Polar and azimuth iterations continue alternately until the eigenray is determined within the desired angular tolerance. This process yields an eigenray and allows for analysis of apparent directivity.

2.3 Simulation

With the eigen-ray solving framework described above, a simulation was carried out using a typical trajectory for a launch from Vandenberg Space Force Base (for this paper the trajectory for the Starlink mission 5-13 was used as provided by the base). 56 simulated stations were positioned along the north, northeast, east, southeast, south, southwest, west, and northwest headings to the launch pad in order to get a range of different headings. These stations were arranged at varying distances ranging from 1 km to 15 km to span a representative range for typical acoustic measurements. Eigenrays were found from the trajectory for each of these simulated stations for 12 different dates (1 for each month of the year) for diurnal weather data as measured by weather balloons launched on base. By simulating these eigenrays, the difference between the initial angle of the eigenray and the straight ray connecting the trajectory to the receiver can be determined. Figure 2.2 shows a layout of simulated station locations.

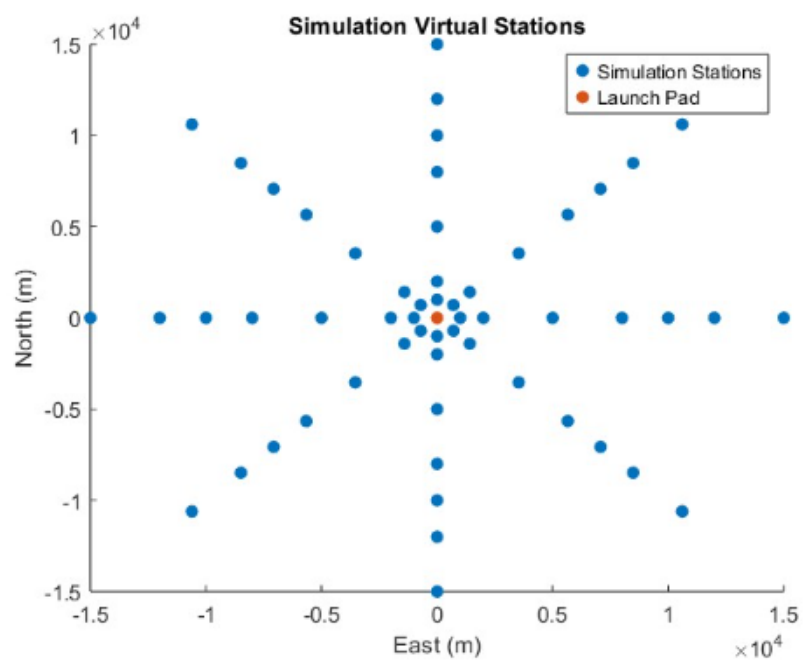


Figure 2.2 Layout of the 56 simulated receiver stations around the launch pad at Vandenberg Space Force Base. Stations are positioned along eight azimuthal directions (N, NE, E, SE, S, SW, W, NW) at distances from 1 km to 15 km. This configuration allows analysis of apparent directivity across range with a representative collection of stations in the azimuth.

Chapter 3

Results

The following section presents the results of the eigenray simulations described in Section 2, with emphasis on quantifying how atmospheric refraction alters the apparent launch angles of acoustic rays relative to straight-line propagation. Using the iterative eigenray solver, ray paths were computed from the launch trajectory to 56 receiver locations spanning eight azimuthal directions and ranges from 1 to 15 km, under diurnal atmospheric conditions for twelve representative days of the year. These results are used to understand how atmospheric refraction can affect assumed initial directivity as well as how distance from the launch pad influence these effects.

The peak directivity for rocket noise typically falls within the 60-80° range [11–14]. Therefore, we will examine simulation results considering only rays that fall within this range according to the straight-ray model as these represent the peak levels that will be measured for a rocket launch. Figure 3.1 shows the differences in apparent launch angle between the straight-ray model and the eigenray model for all rays traced to all stations across all simulation days within the 60–80° range. The mean deviance between the two models was 2.58°.

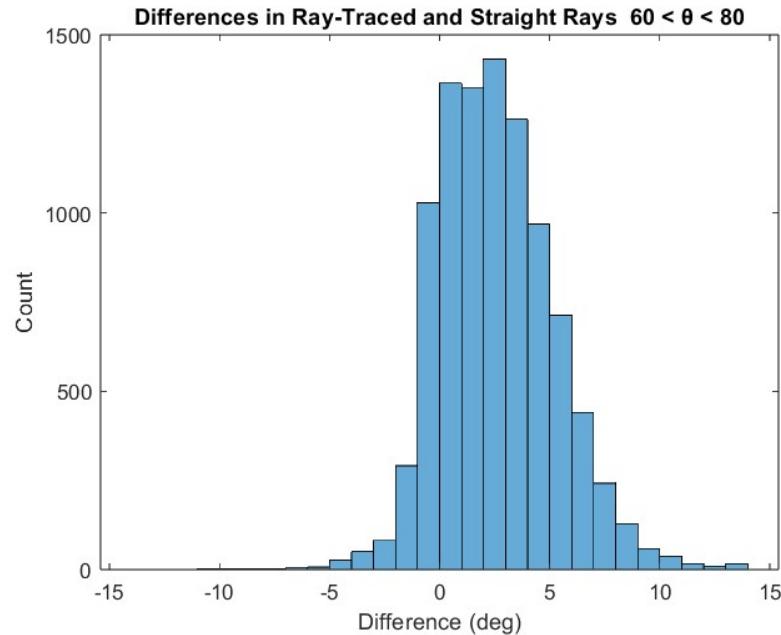


Figure 3.1 Histogram of angular deviations between straight-line propagation and ray-traced eigenrays for rays within the 60–80° launch angle range. Positive values indicate rays bent upward, and negative values indicate downward bending relative to the straight-ray assumption. The mean deviation is 2.58°, demonstrating measurable atmospheric effects even at short ranges.

3.0.1 Range Dependence

In this subsection we will analyze how the distance of receiver stations from the launch pad influences angular deviance. Stations were grouped by radial distance, ranging from 1 km to 15 km. The angular deviations between the straight-ray and eigenray models were calculated for each distance group to examine how atmospheric refraction affects apparent launch angles. Table 3.1 summarizes the results for the representative trajectory considering only rays within the 60–80° range.

Table 3.1 Mean and standard deviation of angular deviation between straight-line propagation and ray-traced eigenrays for receiver stations at various distances from the launch pad. Values are calculated for rays within the 60–80° launch angle range.

Distance (km)	Mean Deviance (deg)	Std (deg)
1	2.4	2.98
2	2.2	2.48
5	1.8	1.99
8	2.3	2.26
10	2.7	2.40
12	3.0	2.55
15	3.3	3.13

Chapter 4

Discussion

Previous studies have demonstrated the use of measured rocket acoustic directivity to infer source parameters, including sound power and radiation patterns [11] [12] [13]. These works typically rely on far-field measurements and assume simple propagation models to reconstruct source characteristics. Our study builds on this approach by highlighting how atmospheric effects, such as temperature and wind gradients, can significantly modify the apparent directivity observed at different stations. Incorporating ray-tracing models into this framework could provide a more accurate interpretation of field data and refine the reconstruction of source parameters compared to straight-ray assumptions alone.

Contrary to intuition, the deviation in apparent directivity does not increase monotonically with distance. Close stations can exhibit substantial deviations due to strong atmospheric gradients near the surface. Although these rays travel shorter distances, a significant portion of their path passes through regions of sharp curvature, producing measurable shifts in apparent launch angle even within 1 km of the pad.

Temperature gradients are likely to be the driving factor behind the mean differences in apparent directivity, where wind is likely the driving factor in the spread. This is because temperature affects

the curvature of all rays in all directions equally (all rays bend up or down). The wind does not, and is therefore responsible for the variation seen in the bending rays.

4.1 Sources of Uncertainty

While the current study demonstrates the importance of atmospheric effects on apparent directivity, several limitations should be noted. The atmospheric profiles used may not capture small-scale or rapidly changing conditions. In addition, no probabilistic analysis was performed. All atmospheric profiles were treated as representative of the whole area, when in reality they only represent a vertical slice of the atmosphere. Implementing atmospheric weather models instead of profiles interpolated from measured radiosonde data might yield different results. The ray-tracing method neglects diffraction and nonlinear acoustic effects. Finally, validation against direct field measurements is needed to confirm the accuracy of the modeled apparent directivity differences. These factors suggest that while the trends identified are robust, absolute values should be interpreted with caution.

Chapter 5

Conclusion

This study demonstrates that atmospheric effects, specifically temperature gradients and wind, have a significant impact on the apparent directivity of acoustic sources inferred from field measurements. Straight-ray assumptions introduce systematic biases dependent on distance from the launch pad.

These results underscore the necessity of incorporating atmospheric ray-tracing models when reconstructing source directivity from acoustic measurements, particularly in environments with strong thermal or wind stratification. Accounting for these effects improves the accuracy of source characterization, enhances predictive models for launch noise, and provides a framework for interpreting acoustic data in complex atmospheric conditions. Accurate estimation of apparent directivity is critical for constructing empirical source models for rockets and predicting levels even at short ranges.

Future work could include dynamic ray-tracing formulations to determine amplitude corrections and a direct comparison of ray-tracing and straight-ray models against measured data to further validate and refine source reconstruction methods. Additionally, using weather models outside of radiosonde measured data could lead to different results when the time of the launch differs from the time the balloon is launched.

Bibliography

- [1] I. Klotz, “Global Orbital Launch Attempts Surpass Records in 2024–2025,” *Aviation Week & Space Technology* (2026), global orbital launch attempts reached 329 in 2025, up about 25% from the previous year, with SpaceX conducting a record 165 Falcon9 flights.
- [2] “SpaceX Starship/Super Heavy Cape Canaveral Space Force Station Draft Environmental Impact Statement – Noise Report,”, 2025, discusses structural damage potential from high acoustic levels, noting most susceptible elements and overpressure thresholds.
- [3] F. A. Administration, “Draft Environmental Impact Statement for Space Launch Noise: Structural and Community Effects,” Technical report, FAA, (2025) , summarizes relationship between acoustic levels and structural damage claims.
- [4] R. W. Peverly, “Determination of Rocket Engine Noise Damage to Community Dwellings Near Launch Sites, Volume I,” Technical Report No. NASA-CR-64284, NASA, (1964) , contractor report defining noise damage thresholds for residential structures.
- [5] N. Aeronautics and S. Administration, “Launch Noise Study for the Wallops Flight Facility Launch Vehicle Noise Studies,”, 2019, noise propagation in the model assumes straight-line sound path between source and receiver for rocket launch noise prediction.

- [6] N. Aeronautics and S. Administration, “Final Environmental Assessment for Atlas V/Vulcan Centaur Launches: Noise Modeling,” 2019, launch noise model assumes straight-line propagation between source and receiver.
- [7] A. D. Pierce, *Acoustics: An Introduction to Its Physical Principles and Applications* (Acoustical Society of America & American Institute of Physics, New York, 1989), comprehensive graduate-level textbook covering fundamental acoustics theory and wave propagation.
- [8] P. Schäfer and M. Vorländer, “Atmospheric Ray Tracing: An efficient, open-source framework for finding eigenrays in a stratified, moving medium,” *Acta Acust.* **5**, 26 .
- [9] I. Durre, X. Yin, R. S. Vose, S. Applequist, J. Arnfield, B. Korzeniewski, and B. Hundermark, “Integrated Global Radiosonde Archive (IGRA), Version 2,” NOAA National Centers for Environmental Information (NCEI), Dataset, 2016, quality-controlled radiosonde observations of temperature, humidity, and winds from globally distributed stations; accessed for atmospheric profile data.
- [10] D. K. Wilson, “Outdoor Sound Propagation Calculator,” in *Acoustics in Moving Inhomogeneous Media, 2nd Edition*, V. E. Ostashev and D. K. Wilson, eds., (Taylor & Francis, Boca Raton, FL, 2015), mATLAB application used for validation of ray-tracing code.
- [11] M. C. Anderson, L. T. Mathews, R. Rasband, and K. L. Gee, “Frequency-Dependent Directivity and Sound Power Measurements of Two Launched United Launch Alliance Atlas V Rockets,” *Acoustics and Ultrasonics* (2023), reports directivity curves from multiple microphone positions around Atlas V launches.
- [12] G. W. Hart, K. L. Gee, E. G. Hintz, N. F. Carlston, G. G. Nuccitelli, and T. Mahlmann, “Using photographs to verify the nature of Mach wave radiation from a Falcon 9 rocket plume,” In *Proceedings of Meetings on Acoustics*, **54**, 040012 (Acoustical Society of America,

2025), presented at the 186th Meeting of the Acoustical Society of America and the Canadian Acoustical Association, Ottawa, Ontario, Canada, May 2024.

- [13] L. T. Mathews, G. W. Hart, K. L. Gee, C. F. Cunningham, and M. C. Anderson, “Characterization of Falcon 9 Launch Vehicle Noise from Far-Field Measurements,” *The Journal of the Acoustical Society of America* **150**, 620–632 (2021), shows measured rocket noise characteristics including overall directivity and connections to Mach number.
- [14] M. G. Yancey, I. R. Jackson, G. W. Hart, L. T. Mathews, and K. L. Gee, “A Study of Rocket Launch Directivity and the Potential Correlation of Various Parameters,” *The Journal of the Acoustical Society of America* (2023), provides directivity measurements for rocket launches and examines how parameters like Mach number influence radiation patterns.

Index

Apparent Directivity, ii
Atmospheric Refraction, 1

Eigenray, 5

Radiosonde, 5

Ray, 1

Ray Tracing, 1

Simulation, 7

Slowness, 4

Temperature Gradient, 1

Wind Gradient, 1